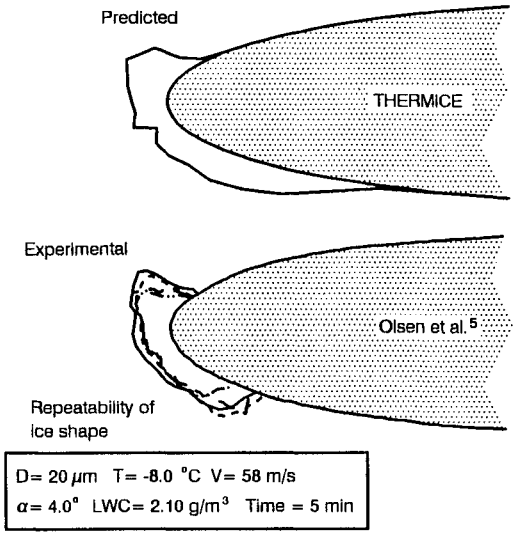

Fig. 3 Comparison of computed and experimental ice shapes in glaze ice conditions ($T = -8°C$).

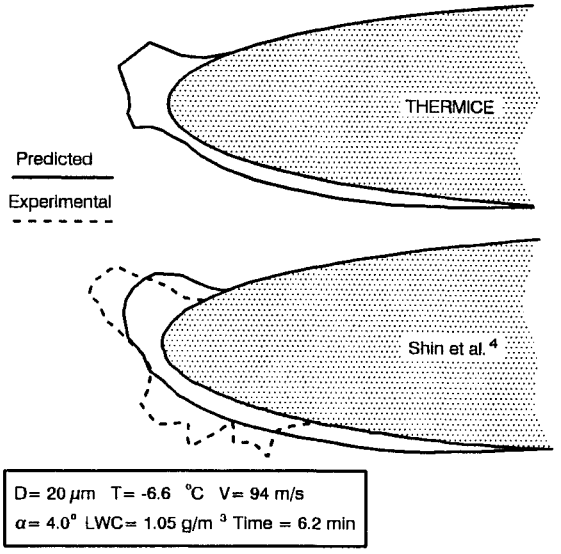

Fig. 4 Comparison of computed and experimental ice shapes in glaze ice conditions ($T = -6.6°C$).

on the energy balance. The continuity and energy equations are given by

$$\dot{m}_{im} + \dot{m}_{in} = \dot{m}_{va} + \dot{m}_{ou} + \dot{m}_{so} \tag{2}$$

$$\dot{E}_{so} + \dot{H}_{va} + \dot{H}_{ou} - \dot{H}_{in} - \dot{H}_{im} = \dot{Q}_f - \dot{Q}_c \tag{3}$$

Enthalpy and internal energy are calculated in relation to a given reference state and depend on the type of surface involved, whereas the heat transfer coefficient is computed from two relations, one for the laminar region and one for turbulent region.[3] The roughness model used is based on empirical relation as given by Ref. 4.

Results and Discussion

THERMICE has been tested in rime and glaze ice conditions and compared with experimental data and numerical results. Figures 1 and 2 show comparison between results calculated with THERMICE and those given by Shin et al.[4] in rime ice conditions. The calculated ice shape compares well with experimental data, particularly for the impingement limits on the upper and lower surface of the airfoil. Figure 3 shows comparison with a series of experiments conducted by Olsen et al.[5] in glaze ice conditions. We can observe that the horn is well-predicted, but the lower impingement limit, and consequently the accumulated mass of ice, is overestimated. Finally, Fig. 4 shows the resulting ice shape compared with experimental and numerical results at a temperature of $-6.6°C$. The results obtained with THERMICE compare well with the numerical data, but the experimental ice shape is not well-reproduced. This is the weakness of icing codes to predict glaze ice shape since there is limited understanding of the physical phenomenon of rough surfaces. Thus, it will be helpful if some experimental data could be obtained for heat transfer and roughness characterization.

Conclusions

An icing code including thermodynamic effects has been developed. It predicts well ice accretion in rime ice conditions. However, for glaze ice the results do not agree well with experimental data. For a realistic ice accretion it is important to include the microphysical aspect of ice, model accurately the convective heat transfer, and improve the correlations of equivalent sand-grain roughness.

Acknowledgment

The authors would like to acknowledge the support provided by Bombardier Inc./Canadair.

References

[1]Brumby, R. E., "Effects of Adverse Weather on Aerodynamics," *Proceedings of the Panel Specialists Meeting* (Toulouse, France), 1991, pp. 2.1–2.4 (AGARD CP 496).

[2]Mavriplis, F., "Icing and Contamination of Aircraft Surfaces: Industry's Concerns," *Proceedings of the First Bombardier International Workshop on Aircraft Icing and Boundary-Layer Stability and Transition*, edited by I. Paraschivoiu, Ecole Polytechnique de Montreal, Canada, 1993, pp. 51–55.

[3]Brahimi, M. T., Tran, P., and Paraschivoiu, I., "Numerical Simulation and Thermodynamic Analysis of Ice Accretion on Aircraft Wings," C.D.T., École Polytechnique de Montréal, Project C128, Canadair, Montreal, Canada, May 1994.

[4]Shin, J., Berkowitz, B., Chen, H., and Cebeci, T., "Prediction of Ice Shapes and Their Effect on Airfoil Drag," *Journal of Aircraft*, Vol. 31, No. 2, 1994, pp. 263–270.

[5]Olsen, W., Shaw, R., and Newton, J., "Ice Shapes and the Resulting Drag Increase for NACA 0012 Airfoil," NASA TM 83556, Jan. 1984.

Applicability of Newtonian and Linear Theory to Slender Hypersonic Bodies

Steven P. Kuester* and John D. Anderson Jr.†
University of Maryland,
College Park, Maryland 20742

Introduction

FOR many years, fluid dynamicists have looked for simple expressions to characterize aerodynamic properties for specific flow regimes. This has resulted in such expressions as the Prandtl-Glauert rule for subsonic lift coefficient ap-

Received April 11, 1994; revision received May 31, 1994; accepted for publication May 31, 1994.

*Graduate Research Assistant, Department of Aerospace Engineering, Bldg. 382. Student Member AIAA.

†Professor Aerospace Engineering, Department of Aerospace Engineering, Bldg. 88. Fellow AIAA.

proximations, and Prandtl's lifting-line theory for finite wings in an incompressible fluid. Similarly, Newton's "sine-squared" law can be used to approximate the flow about bodies traveling at hypersonic velocities. The question exists as to what extent these approximations become valid or whether better approximations exist. The goal of this research has been to assess the accuracy of Newtonian theory for application to slender hypersonic bodies and to investigate whether linear theory can be used to provide accurate approximations for similar cases (we recognize that linear theory is theoretically not valid for hypersonic flow, but the intent is to define conditions, if any, that give reasonable engineering results). The approach has been to calculate the pressure distribution over a biconvex two-dimensional model by using Newtonian and linearized theory, and to compare them with an exact computation fluid dynamics (CFD) solution of the two-dimensional Euler equations for steady, inviscid, irrotational flow.

Techniques

MacCormack's downstream marching CFD technique was used to obtain the exact pressure distribution over a biconvex airfoil by numerically solving the governing equations of the flow at a distinct set of points. MacCormack's technique is a downstream marching, finite difference method based on a predictor and a corrector step that gives second-order accuracy.[1] Because of the weak shocks associated with slender biconvex shapes, MacCormack's technique is an acceptable method for solving the flow equations for the cases investigated, and theoretically approaches the exact solution as the grid spacing approaches zero. This convergence is conditional upon the stability of the calculation that can be insured by maintaining the downstream grid spacing within the Courant-Friedrichs-Lewy stability criterion. The computational grid lies between the leading-edge oblique shock, and the body and the boundary conditions are found by using the oblique shock relations at the shock and Prandtl-Meyer expansion/compression at the body. Software was written in C and run on a personal computer to implement MacCormack's CFD technique, and to numerically integrate the coefficient of pressure over the entire surface of the body. These calculations produced the coefficient of lift, coefficient of drag, and lift-to-drag ratio for each of the three computational methods (exact CFD, linear approximation, and Newtonian approximation). Validation of the CFD code was performed by calculating the flow over a wedge at various angles of attack, thickness to chord ratios t/c, and Mach numbers, and by comparing the CFD results with theoretical results. Results from these tests verify that the CFD algorithm is capable of producing an accurate representation of the pressure distribution.

It is generally assumed that linear theory is only valid up to Mach 5 (the beginning of the hypersonic flow regime), but few quantitative results have been found to confirm this.[2] Therefore, it still is an academic problem to determine quantitatively over what Mach number ranges linear theory is valid for slender bodies. Although this research has focused on slender bodies ($t/c < 0.5$), it is acknowledged that linear (and Newtonian) theory may be valid for different Mach ranges for thicker bodies. In summary, linearized flow is a closed form solution to a linear approximation of the nonlinear governing Euler equations.[3] The linearization of the governing equations is based upon the assumption that perturbation velocities to the freestream velocity are negligible and, therefore, can be ignored to represent the governing equations as a solvable linear partial differential equation. This equation leads to an expression for the coefficient of pressure at a point in the flow [Eq. (1)] and can be numerically integrated over the surface of the body to give approximations for C_l, C_d, and L/D:

$$C_p = 2\theta/\sqrt{M_\infty^2 - 1} \tag{1}$$

Similar to linear theory, Newton's "sine-squared" theory has been found to be a fair approximation for only a certain set of conditions. Specifically, Newtonian theory has generally been accepted to be a fair approximation for hypersonic bodies with strong leading-edge shocks such as blunt bodies and thick airfoils[4,5] (oblique shock theory predicts that Newton's approximation becomes more accurate as the density behind the shock becomes larger, i.e., the shock becomes stronger). However, there is some reason to believe that Newtonian theory is not valid for weaker shocks associated with slender bodies but, once again, little research has been found to support this. This is the reason for examining the validity of Newtonian theory for slender hypersonic bodies. In summary, Newtonian theory states that the normal momentum of flow impacting a surface is transferred to the body while the tangential component is conserved.[6] This leads to the result that the coefficient of pressure on the surface of the body is exclusively a function of the angle between the tangent of the body and the freestream velocity [Eq. (2)]:

$$C_p = (p - p_\infty)/\tfrac{1}{2}\rho v_\infty^2 = 2 \sin \theta \tag{2}$$

Results

Computations of three parameters (coefficient of lift, coefficient of drag, and lift-to-drag ratio) are tabulated for both

Table 1 Coefficient of lift and related errors from exact CFD solution, linear theory, and Newtonian theory for various Mach numbers and angle of attacks

	C_l, $t/c = 0.05$				
	CFD	Linear	Percentage difference	Newton	Percentage difference
$M = 5$, deg					
$\alpha = 0$	0.00000	0.00000	—	0.00000	—
$\alpha = 0.9$	0.01331	0.01278	3.98	0.00313	76.46
$\alpha = 1.8$	0.02670	0.02557	4.23	0.00642	75.97
$\alpha = 2.7$	0.04022	0.03836	4.62	0.00999	75.16
$M = 7.5$, deg					
$\alpha = 0$	0.00000	0.00000	—	0.00000	—
$\alpha = 0.9$	0.00921	0.00843	8.49	0.00313	65.97
$\alpha = 1.8$	0.01851	0.01686	8.91	0.00642	65.34
$\alpha = 2.7$	0.02799	0.02528	9.68	0.00999	64.30
$M = 10$, deg					
$\alpha = 0$	0.00000	0.00000	—	0.00000	—
$\alpha = 0.9$	0.00731	0.00629	13.95	0.00313	57.16
$\alpha = 1.8$	0.01475	0.01259	14.64	0.00642	56.51
$\alpha = 2.7$	0.02241	0.01888	15.75	0.00999	55.41
$M = 12.5$, deg					
$\alpha = 0$	0.00000	0.00000	—	0.00000	—
$\alpha = 0.9$	0.00628	0.00503	20.00	0.00313	50.14

Table 2 Coefficient of drag and related errors from exact CFD solution, linear theory, and Newtonian theory for various Mach numbers and angle of attacks

	C_D	$t/c = 0.05$			
	CFD	Linear	Percentage difference	Newton	Percentage difference
$M = 5$, deg					
$\alpha = 0$	0.00278	0.00272	2.16	0.00050	82.14
$\alpha = 0.9$	0.00300	0.00292	2.54	0.00057	80.98
$\alpha = 1.8$	0.00365	0.00352	3.45	0.00079	78.28
$\alpha = 2.7$	0.00474	0.00452	4.54	0.00118	75.20
$M = 7.5$, deg					
$\alpha = 0$	0.00188	0.00179	4.73	0.00050	73.60
$\alpha = 0.9$	0.00204	0.00192	5.45	0.00057	72.00
$\alpha = 1.8$	0.00250	0.00232	7.31	0.00079	68.35
$\alpha = 2.7$	0.00329	0.00298	9.45	0.00118	64.30
$M = 10$, deg					
$\alpha = 0$	0.00146	0.00134	8.03	0.00050	65.92
$\alpha = 0.9$	0.00158	0.00144	9.11	0.00057	63.97
$\alpha = 1.8$	0.00197	0.00173	11.89	0.00079	59.74
$\alpha = 2.7$	0.00262	0.00223	15.17	0.00118	55.22
$M = 12.5$, deg					
$\alpha = 0$	0.00121	0.00107	11.58	0.00050	58.92
$\alpha = 0.9$	0.00132	0.00115	13.23	0.00057	56.94

Table 3 Lift-to-drag ratio and related errors from exact CFD solution, linear theory, and Newtonian theory for various Mach numbers and angle of attacks

	L/D	$t/c = 0.05$			
	CFD	Linear	Percentage difference	Newton	Percentage difference
$M = 5$, deg					
$\alpha = 0$	0.00000	0.00000	—	0.00000	—
$\alpha = 0.9$	4.44259	4.37671	1.48	5.49939	−23.79
$\alpha = 1.8$	7.32109	7.26214	0.81	8.09668	−10.59
$\alpha = 2.7$	8.48881	8.48110	0.09	8.50383	−0.18
$M = 7.5$, deg					
$\alpha = 0$	0.00000	0.00000	—	0.00000	—
$\alpha = 0.9$	4.52432	4.37890	3.21	5.49939	−21.55
$\alpha = 1.8$	7.39513	7.26724	1.73	8.09668	−9.49
$\alpha = 2.7$	8.50501	8.48322	0.26	8.50383	0.01
$M = 10$, deg					
$\alpha = 0$	0.00000	0.00000	—	0.00000	—
$\alpha = 0.9$	4.62619	4.37996	5.32	5.49939	−18.88
$\alpha = 1.8$	7.49492	7.26067	3.13	8.09668	−8.03
$\alpha = 2.7$	8.54040	8.48158	0.69	8.50383	0.43
$M = 12.5$, deg					
$\alpha = 0$	0.00000	0.00000	—	0.00000	—
$\alpha = 0.9$	4.74981	4.37892	7.81	5.49939	−15.78

approximation methods and exact CFD results as a function of Mach number and angle of attack (see Tables 1–3). Included are the percentage differences of the approximations from the exact values. All these cases were for a thickness-to-chord ratio of 5% ($t/c = 0.05$). It should be noted that the thickness-to-chord ratio could be considered to be another independent variable. But, it can be observed that increasing it is similar to increasing the Mach number. This is understandable because they both serve the purpose of strengthening the leading-edge shock. Therefore, only one needs to be an independent variable.

Several trends can be observed in the results presented in Tables 1–3. First, Newtonian theory is not a good approximation for both the coefficients of lift and drag (50–80% errors). This is understandable because oblique shock theory shows that Newtonian theory is not as accurate for weaker oblique portions of leading-edge shocks than as for the stronger normal shock portions. From the previous discussion of thickness-to-chord ratio it can be inferred that for even more slender bodies the effect is similar to decreasing the Mach number and, therefore, the Newtonian approximation would be even worse. Unlike C_l and C_d, the results of the Newtonian approximation for predicting the lift-to-drag ratio are quite a surprise; they give more accurate approximations in all cases and even acceptable engineering approximations ($<\sim 10\%$ error) in cases of higher angles of attack (>1.8 deg). The reason for inaccuracy in the coefficients of lift and drag, but accuracy in their ratio (L/D), may be that errors in the pressure distribution are negated when taking their ratio. Another trend of interest is that linear theory produces accurate approximations for all three parameters, for almost all cases below Mach number 10. Once again, using this trend and our discussion about thickness-to-chord ratios earlier, we would expect linear theory to be even more accurate for more slender bodies. Linear theory may give good approximations above Mach 5 because perturbation velocities are small due to the slenderness of the body.

Concluding Remarks

Newtonian theory generally is not a good approximation of slender hypersonic bodies. There is one exception: Newtonian approximations of the lift-to-drag ratio give reasonable engineering results. For rough engineering calculations, it is more appropriate to use a lift-to-drag ratio as a characterizing parameter than the coefficients of lift or drag. Furthermore, this research has shown that a more practical upper limit of linear theory approximations is Mach 10 for slender ($t/c < 5\%$) bodies.

References

[1]MacCormack, R. W., "The Effect of Viscosity in Hypervelocity Impact Cratering," AIAA Paper 69-354, April 1969.

[2]Anderson, J. D., *Modern Compressible Flow with Historical Perspective*, McGraw-Hill, New York, 1984, p. 255.

[3]Anderson, J. D., *Modern Compressible Flow with Historical Perspective*, McGraw-Hill, New York, 1984, pp. 251–277.

[4]Anderson, J. D., *Fundamentals of Aerodynamics*, McGraw-Hill, New York, 1984, pp. 370–380.

[5]Hankey, W. L., *Re-Entry Aerodynamics*, AIAA Education Series, AIAA, Washington, DC, 1988, pp. 62–64.

[6]Anderson, J. D., *Fundamentals of Aerodynamics*, McGraw-Hill, New York, 1984, pp. 483–487.

Aerodynamic Characteristics of Vortex Flaps on a Double-Delta Planform

Lance W. Traub*
University of the Witwatersrand, Johannesburg, South Africa

Introduction

NUMEROUS investigations have shown the leading-edge vortex flap[1–6] (LEVF) concept to be effective in reducing drag. The LEVF works by concentrating the suction of the leading-edge vortex on the flap, which may with suitable orientation, result in a thrust force. Thus, cruise and maneuver performance may be improved. For full thrust recovery, flow reattachment should ideally occur at the flaps hinge line. Recent studies of vortex flaps include improvement in area efficiency and planform,[4] hinge-line sweep, and flap deflection angle,[6] etc. Various flap types have also been investigated, e.g., upper and lower surface, folding or hinged, cavity vortex flaps, as well as apex fences,[6] etc. Tabbed vortex flaps have also been examined as a means to augment vortex induced thrust on the flap.[5] The interaction of LEVFs and trailing-edge flaps has also been studied.[3]

Double-delta or slender cranked wings received considerable attention in the mid-1970s with the development of the "supercruiser" fighter. This aircraft was to have efficient supersonic performance coupled with competitive subsonic maneuverability. The purpose of the double delta was to provide a highly swept inboard panel to meet the supersonic cruise requirement, while the outer lesser swept panel increased the wingspan and improved the subsonic aerodynamic efficiency, as well as handling.[7] Vortex flaps have been tested on some of the proposed supercruiser double-delta configurations.[8] The present investigation is concerned with LEVF effects on a double-delta (or simplified strake-wing) planform.

The model configuration and dimensions are shown in Fig. 1. A LEVF was formed by rotating a 1.1-mm-thick aluminum plate through an angle δ_{FSW} (a downward flap deflection being defined as positive). The vortex flaps were attached to a flat aluminum plate 4.5 mm thick, on which the edges were beveled (Fig. 1). The model had a planform area of 0.13 m^2 (including the flap area), and an aspect ratio of 1.37 with the vortex flaps planar. Only the constant chord vortex flaps as shown in Fig. 1 were tested. The vortex flaps on the strake and wing had an equal planform area of 0.0074 m^2. To facilitate matching the flap areas, the rear delta wing was cropped slightly. The tests were run in the University of the Witwatersrand's low-speed continuous wind tunnel. A freestream velocity of approximately 47 m/s was used. The corresponding Reynolds number based on the wing's root chord was 1.38 $\times$ 10^6. The wind-tunnel balance repeatability for lift, drag, and pitching moment was estimated to be $\Delta C_L = \pm 0.0015$, $\Delta C_D = \pm 0.0008$, $\Delta C_m = \pm 0.0022$.

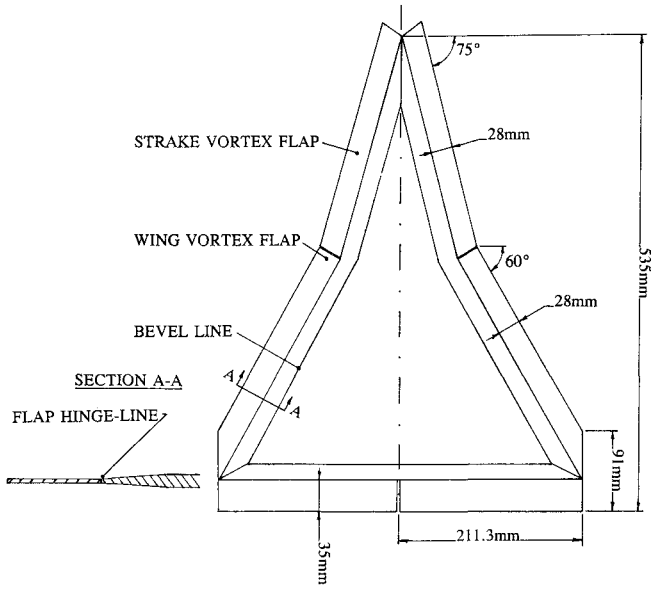

Fig. 1 Model configuration and dimensions.

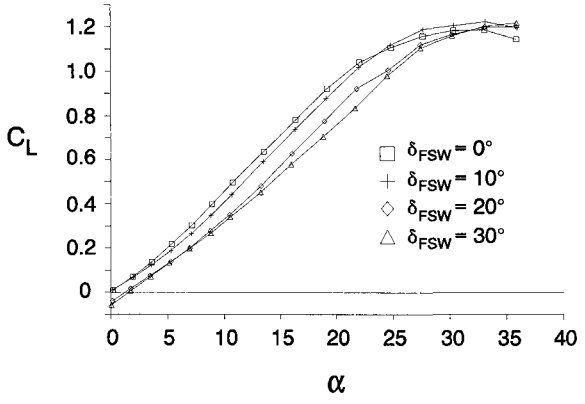

Fig. 2 Effect of vortex flap deflection angle on lift coefficient.

For each respective configuration, the forces and moments were nondimensionalized by the strake-wing area plus the projected vortex flap area. Moments were taken about a point located at 58% of the total root chord (535 mm). All the coefficients were corrected for blockage and interference effects using the procedure detailed in Ref. 9.

In the investigation the vortex flaps both on the strake and on the wing were deflected to 0, 10, 20, and 30 deg. Figure 2 shows that there is generally a reduction in lift with increasing flap angle as would be expected.[2] This is due mainly to a partial suppression of leading-edge vortex formation as a result of flap deflection,[10] and to a lesser extent the result of vortex being traded for thrust.[4] Increasing flap angle also results in a moderate reduction in the attached flow lift component.[10] Suppression of vortical formation, and the concomitant reduction in vortex strength and, hence, suction, manifests itself in a reduction of the nonlinearity of the lift curve with increasing flap deflection (see Fig. 2). Within the angle-

Received Oct. 28, 1993; revision received June 13, 1994; accepted for publication June 13, 1994.

*Graduate Student, School of Mechanical Engineering, Branch of Aeronautical Engineering, 1 Jan Smuts Ave., P.O. Wits, 2050.